Upconversion and Reduced $^4F_{3/2}$ Upper-State Lifetime in Intensely Pumped Nd:YLF

Intense diode pumping of active elements doped with Nd^{3+} is a common approach to produce efficient, reliable, and compact laser systems. The high quantum efficiency of diode pumping can develop large population inversion densities in the $^4F_{3/2}$ upper level that can be lased at either 1 μm or 1.3 μm.[1,2] The upper-state lifetime τ is an important parameter for engineering such lasers since it affects the achievable stored-energy density for a given pumping scheme and ultimately determines the output energy of the laser. The long $^4F_{3/2}$ upper-state lifetime of Nd:YLF (~520 μs for 1-at.% doping[3,4]) makes it an attractive laser material.

Figure 65.36 depicts several energy-transfer mechanisms active in Nd:YLF that can reduce the effective $^4F_{3/2}$ upper-state lifetime, including concentration quenching and energy-transfer upconversion (ETU). Concentration quenching, or self-quenching, of the upper-state lifetime[5–7] is a well-known cross-relaxation process that limits the benefits of increased dopant levels in Nd:YLF. Close-range multipole or quantum mechanical exchange interactions between ions in the $^4F_{3/2}$ upper state and $^4I_{9/2}$ ground state result in two excitations at intermediate energy levels. The rate of additional loss from the $^4F_{3/2}$ upper state introduced by self-quenching generally increases linearly with dopant concentration. It is shown in this work that significant reductions in the effective upper-state lifetime also result from ETU processes at high population inversion in Nd:YLF. ETU, also known as nonlinear self-quenching, is analogous to self-quenching except interactions between two ions in the $^4F_{3/2}$ upper state promote one ion to a higher-lying energy level at the expense of demoting the other ion to a lower level. In this case, the additional loss rate from the upper state is proportional to the square of the excited-state ion density.

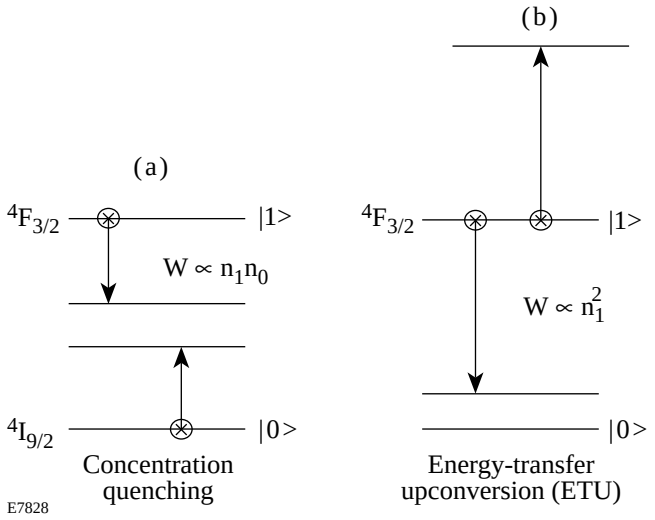

Figure 65.36
Energy-transfer processes introduce additional losses that reduce the effective $^4F_{3/2}$ upper-state lifetime. (a) Concentration quenching rates depend on ground state population densities, n_0, which are equal to doping concentrations under typical operating conditions. (b) Energy-transfer upconversion (ETU) rates depend on the square of the excited-state population density, n_1^2.

In this work, high population inversions are achieved by directly pumping from the ground state into the $^4F_{3/2}$ upper state with an intracavity-pumping arrangement in a tunable, pulsed Cr:LiSAF laser shown in Fig. 65.37. The approximately 1.4-mm-thick, uncoated Nd:YLF sample is placed inside the cavity at Brewster's angle with the pump laser polarization matching the stronger π-polarization absorption[4] in the range of approximately 855 to 885 nm. TEM_{00} mode operation is accomplished with an intracavity aperture in the nearly hemispherical cavity. Typical *Q*-switched pulse lengths were approximately 200 ns (FWHM).

Both a 1053-nm small-signal-gain probe beam and fluorescence, collected at both 1047 and 1053 nm, are used to monitor the population dynamics of the pumped sample. The small-signal-gain probe beam is focused to an approximately 50-μm spot in the center of the pumped region and measured with an amplified silicon diode (Thorlabs PDA150). A 1053±1 nm (FWHM) interference filter and a 2-mm-thick piece of RG-1000 filter glass, along with a small aperture, are used to pass only the 1053-nm probe beam. The small-signal gain is used to measure the absolute $^4F_{3/2}$ upper-state population achieved, given the effective stimulated emission cross section[8] $\sigma_{1053} = 1.9 \times 10^{-19}$ cm^2. The 1-μm fluorescence from the sample is

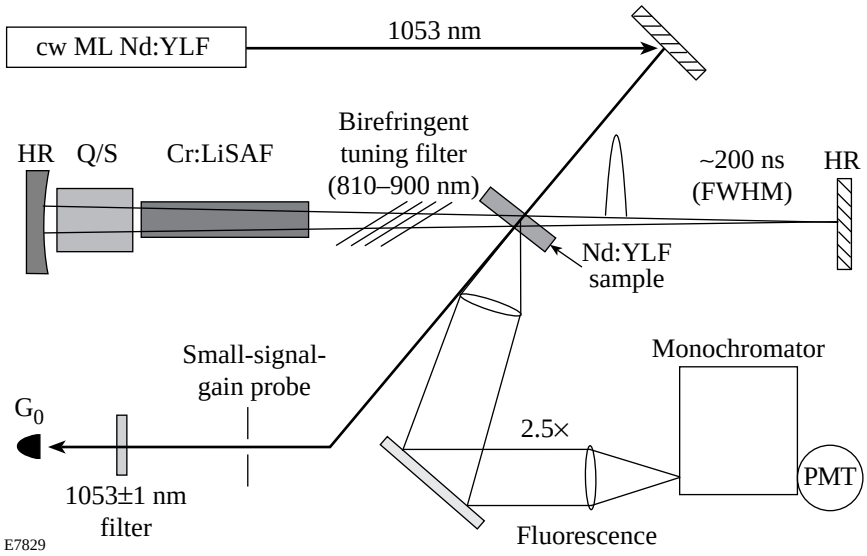

Figure 65.37
An intracavity pumping scheme achieves high population inversions in Nd:YLF. Q/S–Pockels cell *Q*-switch; HR–high-reflector mirrors; PMT–photomultiplier tube; G_0–amplified silicon diode.

collected and imaged onto a 400-μm pinhole to sample approximately the same volume as the small-signal-gain probe. The fluorescence is measured using an S-1 photomultiplier tube (Hamamatsu R5108), cooled to ~0°C, and fitted with a 1051±7.5 nm (FWHM) interference filter and a 2-mm-thick piece of RG-1000 filter glass. Upconversion fluorescence is collected and imaged onto the 250-μm entrance slit of a 1/4-m Jarrel-Ash monochromator and measured using an uncooled, multi-alkali photomultiplier tube (Hamamatsu R928). The 2.5× magnification of the imaging/collection optics effectively samples a 100-μm width around the center of the pumped region.

Figure 65.38 shows the time evolution of the $^4F_{3/2}$ upper-state population normalized to the doping concentration, $n = N/N_{\mathrm{Nd}}$, after intense pumping with an ~200-ns (FWHM) *Q*-switched pulse. At early times when large population inversions exist, there is a strong departure from the simple exponential decay that ultimately occurs at long times and lower inversions. Higher time-resolution measurements show a rapid initial decay consuming approximately 10% of the initial population for times shorter than approximately 10 μs. The horizontal dashed line in Fig. 65.38, representing the approximate maximum upper-state populations achieved in typical flashlamp-pumped Nd:YLF lasers, illustrates that the nonexponential decay associated with the two-body ETU process is observed only at inversion densities typical of intensely diode-pumped lasers.

An ETU loss channel from the $^4F_{3/2}$ upper state is confirmed in the inset to Fig. 65.38, which illustrates upconversion fluorescence measured at approximately 530 nm under similar conditions. Visible fluorescence is also observed near 591 and 665 nm with similar decay dynamics. The long duration and nonexponential nature of this upconversion fluorescence are consistent with several predicted two-body ETU processes[9] that promote ions from the $^4F_{3/2}$ upper-state population to the higher-lying $^4G_{7/2}$ and $^2G_{9/2}$ manifolds. Since the lifetimes of these latter states are very short ($\tau < 10$ ns), no

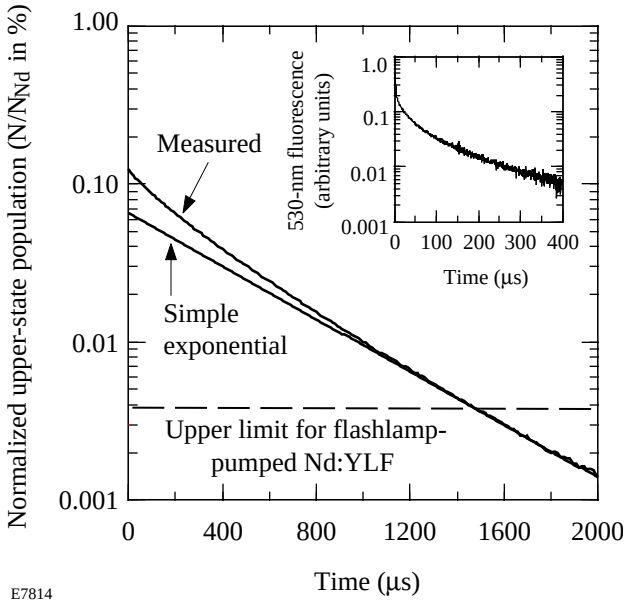

Figure 65.38
Measured population decay of the $^4F_{3/2}$ upper state normalized to the dopant ion concentration. Inset: Visible upconversion fluorescence decay measured under similar experimental conditions.

significant population accumulates in these levels and the resulting fluorescence reflects the ETU rate. The rapid decrease in upconversion fluorescence at early times ($t < 10\ \mu s$) is interpreted as static ETU, while the longer, nonexponential decay is associated with both migration-assisted ETU and the underlying fluorescence decay of the $^4F_{3/2}$ upper state.

Static and migration-assisted ETU can be differentiated by analyzing the nonexponential decay of the $^4F_{3/2}$ upper-state population in coordinates specific to each regime. Following the approach in Ref. 10, the observed decay $n(t)$ is transformed to $\left[n_0 \exp\left(-t/\tau\right)/n(t)\right]-1$ to remove the underlying fluorescent lifetime τ and plotted in Fig. 65.39 versus the coordinates for static and migration-assisted regimes, $\mathrm{erf}\left(\sqrt{t/\tau}\right)$ and $1-\exp\left(-t/\tau\right)$, respectively. The linear relationship for the migration-assisted coordinates is consistent with migration-assisted nonlinear self-quenching of the $^4F_{3/2}$ upper state predicted from the energy-transfer microparameters calculated in Ref. 9. The departure from linearity near the origin in Fig. 65.39 is attributed to the initial phase of static ETU.

The $^4F_{3/2}$ upper-state decay dynamics in Fig. 65.38 can be transformed into a more familiar "rate equation" form

$$\frac{dn}{dt} = -n/\tau - \alpha n^2 - \ldots \qquad (1)$$

by plotting the time derivative dn/dt at each time of the decay versus its corresponding population n. The linear term in Eq. (1) represents the fluorescence lifetime of the $^4F_{3/2}$ upper state, including both radiative and nonradiative decay, and concentration quenching, if present. Quadratic and higher-order terms can be included to represent energy-transfer upconversion processes that consume two or more units of excitation per interaction. A two-body ETU process is included in Eq. (1), as indicated by the quadratic dependence on upper-state population. Normally, the quadratic term would include a factor of 2 to account for the two excitations lost for each ETU interaction; however, for Nd:YLF, ions promoted to higher energy levels rapidly decay back to the $^4F_{3/2}$ upper state by nonradiative processes. Figure 65.40 graphically displays the decay dynamics of Eq. (1) along with a quadratic curve fit that best represents the transformed decay data. The $\tau = 523\ \mu s$ fluorescence lifetime derived from this curve fit matches very well the published values[3,4] for 1-at.% Nd:YLF, while the quadratic coefficient $\alpha = 1.0 \times 10^{-16}$ cm^3/s yields the macroscopic, two-body energy-transfer upconversion coefficient.

The effect of ETU processes on energy storage in Nd:YLF when operating at high population inversions can be estimated by evaluating the "relative" quantum efficiency[5] of the $^4F_{3/2}$ upper state, defined as

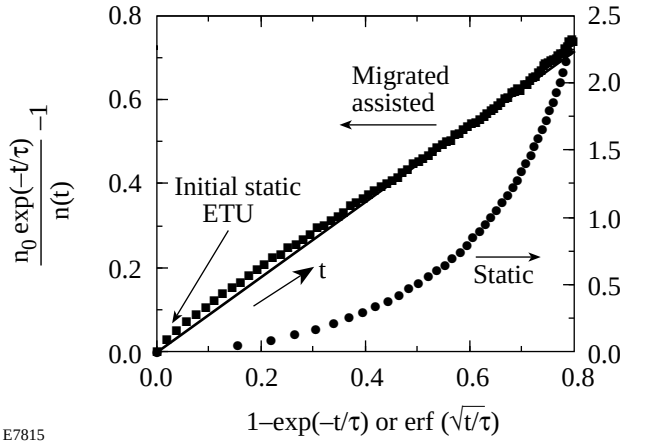

Figure 65.39
The linear dependence of the $^4F_{3/2}$ upper-state decay plotted versus $1 - \exp(-t/\tau)$ indicates migration-assisted ETU. Measurements are equally spaced ($\Delta t = 10\ \mu s$) with time increasing from left to right. An initial phase of static ETU causes the measured plot to depart slightly from Eq. (3), which is also plotted using measured values for α, τ, and n_0.

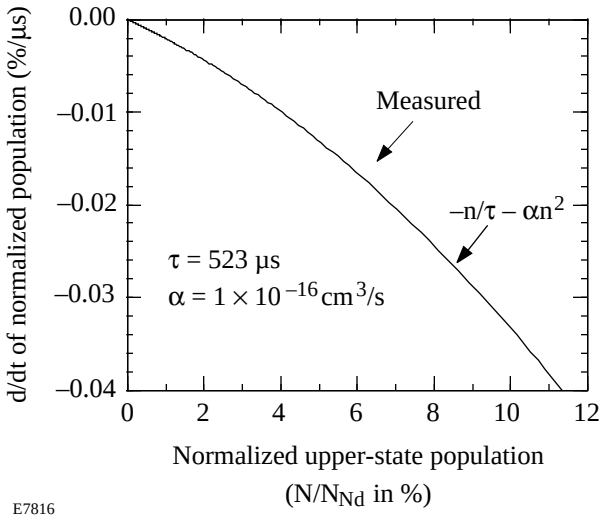

Figure 65.40
Rate equation form for $^4F_{3/2}$ upper-state population decay dynamics shows the quadratic nature of the energy-transfer upconversion (ETU) process active at high population inversions.

$$\eta_{\text{rel}} = \frac{1}{\tau}\int_0^{\infty} \frac{n(t)}{n_0}\,dt, \tag{2}$$

where τ is the fluorescence lifetime. The relative quantum efficiency compares the fluorescence yield of a sample with an initial population n_0 to that expected in the absence of energy transfer. The analytic solution to Eq. (1),[10]

$$n(t) = \frac{n_0 \exp\left(-t/\tau\right)}{1+\alpha\,\tau\,n_0\left[1-\exp\left(-t/\tau\right)\right]} \tag{3}$$

can be substituted into Eq. (2) and integrated to obtain an analytic expression for the relative quantum efficiency

$$\eta_{\text{rel}}\left(n_0\right) = \frac{\ln\left(\alpha\,\tau\,n_0+1\right)}{\alpha\,\tau\,n_0}, \tag{4}$$

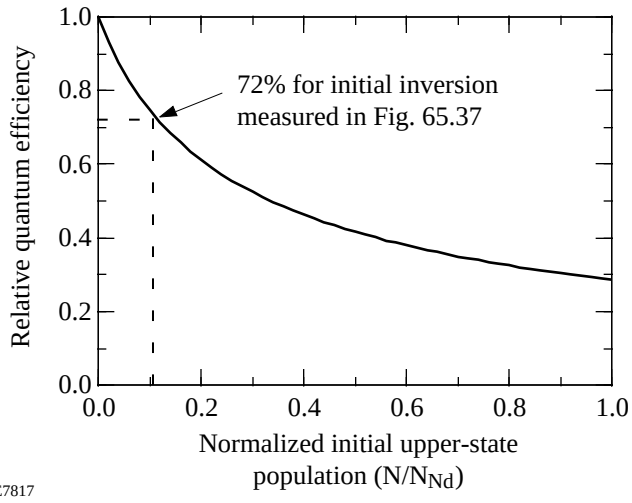

Figure 65.41
Relative quantum efficiency of Nd:YLF under intense pumping calculated using Eq. (4).

which is plotted in Fig. 65.41 using the experimental values for α and τ. A large penalty due to the ETU losses is seen for normalized $^4F_{3/2}$ upper-state populations greater than a few percent. For the experimental conditions in Fig. 65.39, these losses would reduce the relative quantum efficiency to 72%. It should be emphasized that this analysis underestimates the effect of ETU losses since Eq. (1) does not represent well the rapid initial decay due to static ETU or the likely onset of strong three-body ETU processes at high $^4F_{3/2}$ upper-state populations. On the other hand, the above analysis overestimates the effect of the ETU losses on energy storage in real laser systems since it compares the relative importance of ETU processes to fluorescence over an infinite period. An analytical form for storage efficiency[1] appropriate for pumping pulsed lasers is complicated by the nonlinear nature of the $^4F_{3/2}$ upper-state decay dynamics, requiring numerical calculations to evaluate the fraction of pump energy stored in the upper state at the end of a finite pumping period.

ETU losses also negatively impact cw laser performance in active elements operated at high population inversion threshold densities, n_{th}. These losses must be accounted for in an effective saturation intensity,

$$I_{\text{sat}} = h\nu/\sigma\tau_{\text{eff}} = h\nu/\sigma \times \left(1/\tau + \alpha n_{\text{th}}\right),$$

which increases linearly with threshold inversion. Since threshold power is proportional $\left(P_{\text{th}} \propto I_{\text{sat}}\right)$ and slope efficiency is inversely proportional $\left(\eta_{\text{slope}} \propto 1/I_{\text{sat}}\right)$ to the saturation intensity, these important laser operating parameters are adversely affected by increasing threshold densities. Using the experimental values for α and τ in 1-at.% Nd:YLF, a fractional threshold inversion of only 1% increases the effective saturation intensity by more than 7% over its value with no ETU losses.

Increased ETU rates should be observed as the doping concentration increases for several reasons. First, the macroscopic, two-body ETU coefficient, α, increases with doping concentration in the migration-assisted regime since more dopant ions are present on which to migrate. Second, the higher excited-state population densities achievable in higher doped materials and the strong dependence of energy-transfer rates on inter-ion separation lead to an increased contribution of static ETU.

In conclusion, a nonlinear loss channel from the $^4F_{3/2}$ upper state caused by two-body energy-transfer upconversion has been observed in intensely pumped Nd:YLF samples. This loss channel significantly degrades the energy storage capacity and increases the threshold power of Nd:YLF lasers operating at high population inversions.

ACKNOWLEDGMENT

The authors wish to acknowledge Lightning Optical Corporation for providing the Nd:YLF samples and M. A. Noginov for useful discussions. This work was supported by the U.S. Department of Energy Office of Inertial Confinement Fusion under Cooperative Agreement No. DE-FC03-92SF19460 and the University of Rochester.

REFERENCES

1. N. P. Barnes *et al*., IEEE J. Quantum Electon. **26**, 558 (1990).
2. J. R. Lincoln and A. I. Ferguson, Opt. Lett. **19**, 1213 (1994).
3. A. L. Harmer, A. Linz, and D. R. Gabbe, J. Phys. Chem. Solids **30**, 1483 (1969).
4. J. R. Ryan and R. Beach, J. Opt. Soc. Am. B **9**, 1883 (1992).
5. V. Lupei *et al*., Opt. Commun. **60**, 59 (1986).
6. N. P. Barnes, E. D. Filer, and C. A. Morrison, to be published in the *Technical Digest of the Advanced Solid State Laser Conference*, San Francisco, CA (1996).
7. A. A. Kaminskii, *Laser Crystals: Their Physics and Properties*, 2nd ed. (Springer-Verlag, Berlin, 1990), p. 328.
8. E. P. Maldonado and N. D. Vieira, Jr., Opt. Commun. **117**, 102 (1995).
9. A. M. Tkachuk, Opt. Spectrosc. (USSR) **68**, 775 (1990).
10. M. A. Noginov, H. P. Jenssen, and A. Cassanho, in *OSA Proceedings on Advanced Solid-State Lasers*, edited by A. A. Pinto and T. Y. Fan (Optical Society of America, Washington, DC, 1993), Vol. 15, pp. 376–380.